Bioorganic Chemistry 92 (2019) 103198

Contents lists available at ScienceDirect

Bioorganic Chemistry

journal homepage: www.elsevier.com/locate/bioorg

Chemical constituents from *Lonicera japonica* flower buds and their anti-hepatoma and anti-HBV activities

Lanlan Ge[a,b,c,1], Lingyun Xiao[a,b,c,1], Haoqiang Wan[a,d], Jiemei Li[a,d], Kongpeng Lv[b,c], Shusong Peng[d], Boping Zhou[a], Tiyuan Li[e,*], Xiaobin Zeng[a,b,d,*]

[a] Center Lab of Longhua Branch, Shenzhen People's Hospital, 2nd Clinical Medical College of Jinan University, Shenzhen 518120, Guangdong Province, China
[b] Department of Infectious Disease, Shenzhen People's Hospital, 2nd Clinical Medical College of Jinan University, Shenzhen 518120, Guangdong Province, China
[c] Integrated Chinese and Western Medicine Postdoctoral Research Station, Jinan University, Guangzhou 510632, Guangdong Province, China
[d] Department of Pathology (Longhua Branch), Shenzhen People's Hospital, 2nd Clinical Medical College of Jinan University, Shenzhen 518120, Guangdong Province, China
[e] Shenzhen Infectious Disease Medicine Engineering Center, Shenzhen People's Hospital, 2nd Clinical Medical College of Jinan University, Shenzhen 518120, Guangdong Province, China

ARTICLE INFO

Keywords:
Lonicera japonica
Monoterpenoid
Anti-hepatoma activity
Anti-HBV activity

ABSTRACT

Three new naturally occurring monoterpenoids, japopenoid A (**1**), japopenoid B (**23**) japopenoid C (**24**), and one new caffeoylquinic acid derivative (**28**), together with thirty-one known compounds (**2–22**, **25–27**, **29–35**), were isolated and identified from the flower buds of *Lonicera japonica* Thunb. Their structures were determined by extensive 1D and 2D NMR spectroscopic methods, high-resolution mass spectrometry, and the absolute configurations of **1, 23, 24** were determined by comparison of their electronic circular dichroism (ECD) spectrum with literature and theoretical calculation. Structurally, compound **1** is a monoterpenoid featured with an unusual tricyclic skeleton. All compounds (**1–35**) were evaluated for their cytotoxicities against human liver cancer cell lines (HepG 2 and SMMC-7721). Compound **12** exhibited the most potent activity with IC_{50} values of 26.54 ± 1.95 and 8.72 ± 1.57 μg/ml against HepG 2 and SMMC-7721, and the IC_{50} values of compound **13** were 26.54 ± 1.95 and 12.35 ± 1.43 μg/ml, respectively. Western blot results further proved that compound **13** induces hepatoma cell apoptosis *via* the intrinsic apoptosis pathway. In addition, most terpenoids showed inhibitory activity against HBsAg and HBeAg secretion, and HBV DNA replication. In particular, 25 μg/mlof compound **11** inhibits HBsAg and HBeAg secretion, and HBV DNA replication by 39.39 ± 5.25, 15.64 ± 1.25, and 16.13 ± 4.10% compared to the control ($p < 0.05$). These results indicated that *L. japonica* flower buds could be served as functional food for anti-hepatoma and anti-HBV activities.

1. Introduction

Liver cancer is comprised of a malignant tumor that occurs in the liver and represents a major source of morbidity and mortality worldwide [1]. Among primary liver cancers, hepatocellular carcinoma (HCC) represents the major histological type and likely accounts for 70–85% of cases [2]. Cirrhosis precedes most cases of HCC, compared to other causes of cirrhosis, and hepatitis B virus (HBV) infection is associated with a higher risk of developing HCC [3,4]. According to the statistics, HBV infection accounts for up to 54% of HCC cases globally [5]. Since HBV infection is closely related to the occurrence of liver cancer [6], the treatments for HBV and HCC are equally important.

Jin Yin Hua, the flower buds of *Lonicera japonica* Thunb., have been used for traditional Chinese medicine in China or for food therapy (such as tea) in Korea and China for many years [7,8]. Our previous studies have already confirmed that *L. japonica* flower buds contain abundant compounds with anti-HBV and anti-hepatoma activities [9,10]. As part of the ongoing search for promising new anti-HBV and anti-hepatoma compounds from *L. japonica* flower buds, four new compounds (**1**, **23**, **24**, **28**), together with 31 known compounds, were isolated and identified. Their structures were shown in Figs. 1 and 2. The details of the structural determination of new compounds as well as the anti-hepatoma and anti-HBV activities of most compounds are described herein. In addition, Western blot studies were performed to investigate the

* Corresponding authors at: Center Lab of Longhua Branch, Shenzhen People's Hospital, 2nd Clinical Medical College of Jinan University, Shenzhen 518120, Guangdong Province, China (X. Zeng).
E-mail addresses: li.tiyuan@szhospital.com (T. Li), zeng.xiaobin@szhospital.com (X. Zeng).
[1] These authors have contributed equally to this work.

https://doi.org/10.1016/j.bioorg.2019.103198
Received 20 June 2019; Received in revised form 2 August 2019; Accepted 13 August 2019
Available online 16 August 2019
0045-2068/

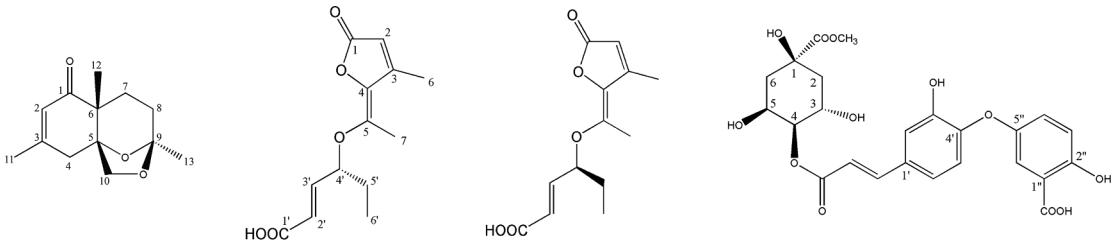

Fig. 1. Chemical structure of newcompounds (**1**, **23**, **24**, and **28**) in *L. japonica* flower buds.

mechanism of action of the active compounds with anti-hepatoma activity.

2. Experiment

2.1. General experimental procedures

Nuclear magnetic resonance (NMR) spectra were recorded on a Bruker DPX-400 spectrometer using standard Bruker pulse programs (Bruker, Karlsruhe, Germany). Chemical shifts are shown as δ-values with reference to tetramethylsilane (TMS) as an internal standard. High-resolution ESI-MS (HR-ESIMS) was measured on a Bruker microTOF-QII mass spectrometer (Bruker, Karlsruhe, Germany). Optical rotations were measured using a WZZ-2B automatic digital polarimeter (Shanghai INESA Physico Optiacal Instrument Co. Ltd., Shanghai, China). UV absorption spectra were recorded on a NanoDrop One^C (Thermo Scientific) from 190 to 850 nm. ECD spectra were recorded on a Chirascan (Applied Photophysics Ltd, England). Sephadex LH-20 (GE, America), silica gel (Qingdao Ocean Chemical Co., Ltd, Qingdao, China), and ODS (40–63 μm, Merck, Darmstadt, Germany) were used for column chromatography. Thin-layer chromatography (TLC) was carried out on silica gel 60 F_{254} (Qingdao Ocean Chemical Co., Ltd., Qingdao, China), and spots were visualized by spraying the plates with 10% H_2SO_4 in EtOH and heating them at 105 °C. Preparative high-performance liquid chromatography (HPLC) was carried out on an EasyChrom 3.2.8.0 system (Guangzhou Ruibai Instrument Technology Co. Ltd., Guangzhou, China) and an octadecyl silica (ODS) column (Cosmosil 5C_{18}-MS-II, 5 μm, 20 × 250 mm, Nacalai Tesque, Kyoto, Japan). The 3-(4,5-Dimethylthiazol-2-yl)-2,5-diphenyltetrazolium bromide (MTT) was purchased from Solarbio (Beijing, China). The anti-human BCL-2, BAX, BAK, and Tublin were obtained from Cell Signaling Technology (Danvers, MA, USA). Diagnostic kits for HBsAg and HBeAg were purchased from Abbott Trading Shanghai Co. Ltd. (Shanghai, China), and a diagnostic kit for HBV DNA was purchased from Hunan Shengxiang Jiancheng Biotechnology Co. Ltd. (Hunan, China). The HPLC-grade methanol was purchased from Sigma-Aldrich Co. (St. Louis, USA). All other analytical chemicals were obtained from Shanghai Chemical Reagents Co., Ltd (Shanghai, China).

2.2. Plant materials

The *L. japonica* flower buds were collected in May 2017 from Pingyi County, Linyi City, Shandong Province, China (Fukangwanjia Pharmaceuticals). The plants were identified by Dr. XB Zeng of Shenzhen People's Hospital and a voucher specimen (No. 20170930) was deposited at Center Lab of Longhua Branch, Shenzhen People's Hospital, Second Clinical Medical College of Jinan University, Shenzhen, China.

2.3. Extraction and isolation

*L. japonic*a flower buds EtOH extract was prepared according to our previous method [9,10]. The EtOH extract was partitioned from with cyclohexane, EtOAc, and *n*-buOH, respectively. The EtOAc fraction yield was 1.3% relative to the dry raw material. Then the EtOAc fraction was divided into 20 fractions (Fractions 1–20) with a silica gel column (5 × 45 cm, 100–200 mesh, CH_2Cl_2–MeOH, 100: 1 → 1: 0, v/v).

Fraction 3 (6.9 g, yellow colloidal) was further chromatographed on the Sephadex LH-20 column (2.3 cm × 75 cm) eluted with CH_2Cl_2–MeOH (8: 2) to afford subfractions 3A–3G *via* thin layer chromatography (TLC). Fr. 3F (2.4 g) was chromatographed on the Sephadex LH-20 column (2.3 × 75 cm) eluted with CH_2Cl_2–MeOH (8: 2) again. Fr. 3F-4 (0.2 g) was subjected to preparative HPLC (Cosmosil 5C_{18}-MS-II, 5 μm, 20 × 250 mm, flow rate: 8 mL/min, wave length: 254 nm, MeOH: H_2O, 53: 47, v/v) yielding compound **1** (2.94 mg, t_R: 21.88 min) and compound **2** (3.64 mg, t_R: 24.80 min). Fr. 3F-5 (0.1 g) was first subjected to the Sephadex LH-20 column chromatography (1.4 × 123.5 cm) isocratic eluted with CH_2Cl_2–MeOH (80: 20, v/v) to afford Fr. 3F-5-1 (100 mg), then compounds **3** (2.40 mg, t_R: 18.48 min) and **4** (1.01 mg, t_R: 26.28 min) were obtained through preparative HPLC (8 mL/min, 254 nm, MeOH: H_2O, 53: 47, v/v) from Fr. 3F-5-1. The subfraction 3G (0.9 g) was further subjected to Sephadex LH-20 column chromatography (1.4 × 123.5 cm) isocratic eluted with CH_2Cl_2–MeOH (80: 20, v/v) to afford 6 subfractions (Fr. 3G-1 to Fr. 3G-6). Fr. 3G-3 (0.3 g) was subjected to the Sephadex LH-20 column chromatography (1.4 × 123.5 cm) isocratic eluted with CH_2Cl_2–MeOH (80: 20, v/v) to afford 6 subfractions (Fr. 3G-3-1 to Fr. 3G-3-6). Fr. 3G-3-2 was separated by preparative HPLC (8 mL/min, 254 nm, MeOH: H_2O, 52: 48, v/v) yielding compounds **5** (1.03 mg, t_R: 11.02 min), **6** (5.01 mg, t_R: 11.68 min), **7** (9.58 mg, t_R: 23.07 min) and **8** (5.60 mg, t_R: 30.28 min). Next, the Fr. 3G-6 (0.1 g) was subjected to the Sephadex LH-20 column chromatography (1.4 × 123.5 cm, CH_2Cl_2–MeOH, 80: 20, v/v) again. The resulting Fr. 3G-6-4 was subjected to preparative HPLC (8 mL/min, 254 nm, MeOH: H_2O, 53: 47, v/v), yielding compounds **9** (7.98 mg, t_R: 11.23 min) and **10** (7.52 mg, t_R: 15.63 min).

Fr. 4 (2.9 g, yellow colloidal) was subjected to the Sephadex LH-20 column chromatography (2.3 × 75 cm) isocratic eluted with CH_2Cl_2–MeOH (80: 20, v/v) to afford 6 subfractions (Fr. 4-1 to Fr. 4-6). The Fr. 4-2 (1.6 g) was subjected to Sephadex LH-20 column chromatography (1.4 × 123.5 cm, CH_2Cl_2–MeOH, 80: 20, v/v) again. And compound **11** (15.12 mg, t_R: 22.83 min) was obtained through preparative HPLC (8 mL/min, 205 nm, MeOH: H_2O, 55: 45, v/v) from Fr. 4-2-2.

Fr. 6 (yellow colloidal, 2.0 g) was separated by Sephadex LH-20 column chromatography (2.3 × 75 cm, CH_2Cl_2–MeOH, 80: 20, v/v) to yield 12 subfractions (Fr. 6-1 to Fr. 6-12). Fr. 6-11 was subjected to preparative HPLC (8 mL/min, 330 nm, MeOH: H_2O, 58: 42, v/v) yielding compounds **12** (0.5 mg, t_R: 20.95 min) and **13** (0.5 mg, t_R: 35.50 min).

Fr. 8 (yellow colloidal, 1.0 g) was submitted to Sephadex LH-20 column chromatography (2.3 × 75 cm) isocratic eluted with CH_2Cl_2–MeOH (80: 20, v/v) to afford 4 subfractions (Fr. 8-1 to Fr. 8-9). Fr. 8-3 was subjected to preparative HPLC (5 mL/min, 254 nm, MeOH: H_2O, 60: 40, v/v) yielding compound **14** (3.37 mg, t_R: 20.30 min). Similarly, subfraction Fr. 8-5 was purified with preparative HPLC (8 mL/min, 205 nm, MeOH: H_2O, 55: 45, v/v) to yield compound **15**

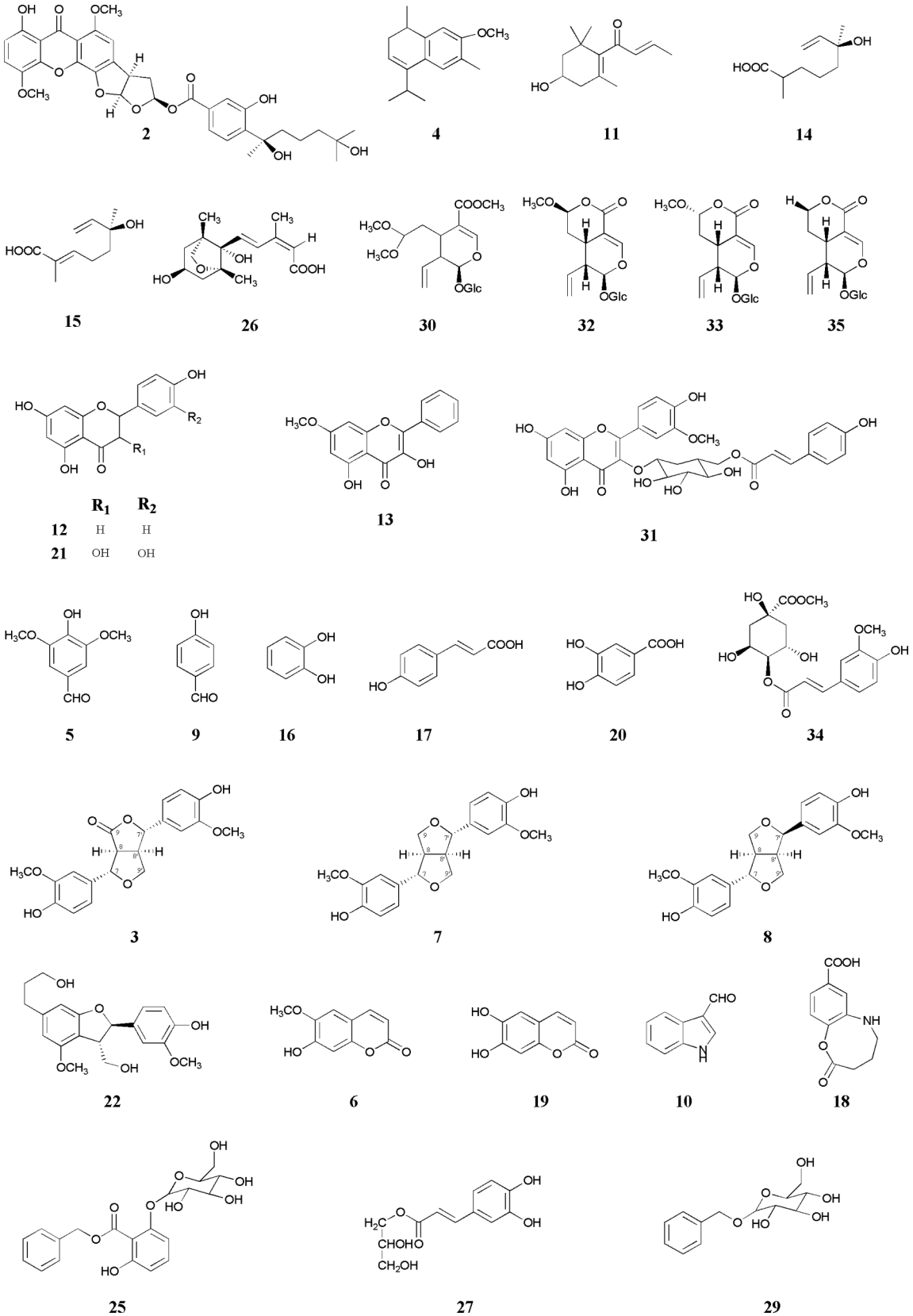

Fig. 2. Chemical structure of other known compounds (**2–22**, **25–27**, and **29–35**) in *L. japonica* flower buds.

(7.05 mg, t_R: 25.54 min). And compound **16** (19.97 mg, t_R: 20.48 min) and compound **17** (12.0 mg, t_R: 31.99 min) were also obtained from Fr. 8-8 by the same method (5 mL/min, 254 nm, MeOH: H_2O, 45: 55, v/v) as outlined above.

Fraction 9 (4.5 g) was chromatographed on the Sephadex LH-20 column (2.3 cm × 75 cm) eluted with CH2Cl2–MeOH (8:2), and then Fr. 9-3 was separated by preparative HPLC (8 mL/min, 254 nm, MeOH: H_2O, 52: 48, v/v) yielding compound **18** (6.63 mg, t_R: 9.44 min).

Fr. 10 (yellow oil, 3.0 g) was submitted to Sephadex LH-20 column chromatography (2.3 × 75 cm) isocratic eluted with CH_2Cl_2–MeOH (80: 20, v/v) to afford 4 subfractions (Fr. 10-1 to Fr. 10-4). Fr. 10-2 was applied to preparative HPLC (8 mL/min, 205 nm, MeOH: H_2O, 30: 70, v/v) and obtain compound **19** (5.83 mg, t_R: 38.26 min). Fr. 10-4 was separated by preparative HPLC (8 mL/min, 254 nm, MeOH: H_2O, 56: 44, v/v) yielding compounds **20** (34.15 mg, t_R: 9.29 min) and **21** (3.23 mg, t_R: 12.81 min), respectively.

Fr. 11 (yellow solid, 3.6 g) was chromatographed on the Sephadex LH-20 column (2.3 cm × 75 cm) eluted with CH_2Cl_2–MeOH (8:2), and then Fr. 11-2 was separated by preparative HPLC (8 mL/min, 205 nm, MeOH: H_2O, 48: 52, v/v) yielding compound **22** (12.14 mg, t_R: 29.36 min). Fr. 11-3 was separated by preparative HPLC (8 mL/min, 254 nm, MeOH: H_2O, 53: 47, v/v), yielding compounds **23** and **24** (10.34 mg, t_R: 8.60 min).

Fr. 12 (yellow solid, 1.2 g) was chromatographed on the Sephadex LH-20 column (2.3 cm × 75 cm) eluted with CH2Cl2–MeOH (8:2), and then Fr. 12-3 was separated by preparative HPLC (8 mL/min, 254 nm, MeOH: H_2O, 60: 40, v/v) yielding compound **25** (6.85 mg, t_R: 11.67 min).

Fr. 13 (yellow solid, 5.5 g) was chromatographed on the Sephadex LH-20 column (2.3 × 75 cm, CH_2Cl_2–MeOH, 80: 20, v/v) to afford subfractions Fr. 13-1 to 13-8 *via* TLC. Compound **26** (11.52 mg, t_R: 29.22 min) was also obtained from Fr. 13-3 by preparative HPLC (5 mL/min, 254 nm, MeOH: H_2O, 42: 58, v/v). Compounds **27** (24.77 mg, t_R: 9.66 min) and **28** (24.20 mg, t_R: 11.22 min) were purified from Fr. 13-4 by preparative HPLC (8 mL/min, 330 nm, MeOH: H_2O, 55: 45 and 45: 55, v/v) twice.

Fr. 14 (yellow solid, 1.6 g) was chromatographed on the Sephadex LH-20 column (2.3 × 75 cm, CH_2Cl_2–MeOH, 80: 20, v/v) to afford subfractions Fr. 14-1 to 14-6 *via* TLC. Fr. 14-4 was separated by preparative HPLC (8 mL/min, 205 nm, MeOH: H_2O, 45: 55, v/v) yielding compounds **29** (9.35 mg, t_R: 12.20 min) and **30** (9.99 mg, t_R: 28.77 min), respectively. And compound **31** (6.46 mg, t_R: 47.78 min) was also obtained from Fr. 14-6 by the same preparative HPLC (8 mL/min, 254 nm, MeOH: H_2O, 55: 45, v/v).

Fr. 15 (yellow solid, 6.0 g) was chromatographed on an ODS column (5.5 × 28 cm) gradually eluted with MeOH–H_2O (10: 90 → 100: 0, v/v) to obtain 6 subfractions (Fr. 15-1 to Fr. 15-6). Fr. 15-4, eluted with MeOH–H_2O (50: 50), was further subjected to preparative HPLC (8 mL/min, 205 nm, MeOH: H_2O, 42: 58, v/v) to yield compounds **32** (7.50 mg, t_R: 18.46 min), **33** (3.55 mg, t_R: 21.96 min) and **34** (11.77 mg, t_R: 31.34 min), respectively.

Fr. 16 (yellow colloidal, 37.0 g), was chromatographed on an ODS column (5.5 × 28 cm) gradually eluted with MeOH–H_2O (10: 90 → 100: 0, v/v) to obtain 9 subfractions (Fr. 16-1 to Fr. 16-9). Fr. 16-3 was subjected to preparative HPLC (Cosmosil 5C_{18}-MS-II, 5 μm, 20 × 250 mm, flow rate: 8 mL/min, wave length: 330 nm, MeOH: H_2O, 35: 65, v/v) yielding compound **35** (127.26 mg, t_R: 24.50 min).

2.4. Spectroscopic data of new compounds

Japopenoid A (**1**). Pale yellow, oil; $[\alpha]_D^{20}$ + 80.3° (c = 0.02, MeOH); UV (MeOH) λ_{max} (logε) 233.5 nm; HR-ESI-MS *m/z* 223.1324 $[M+H]^+$; ^{1}H NMR (400 MHz, d_6-DMSO) and ^{13}C NMR (100 MHz, d_6-DMSO) spectrum information, see Table 1.

Japopenoid B and C (**23** and **24**). Orange oil; $[\alpha]_D^{20}$ 0.0° (c = 0.02, MeOH); UV (MeOH) λ_{max} (logε) 201.5, 288.5 nm; HR-ESI-MS *m/z* 275.1324 $[M+H]^+$; ^{1}H NMR (400 MHz, d_6-DMSO) and ^{13}C NMR (100 MHz, d_6-DMSO) spectrum information, see Table 1.

4-*O*-[4′-*O*-5″-(2,5-dihydroxybenzoic acid)-caffeoyl]-quinic acid methyl ester (**28**). Green oil; $[\alpha]_D^{20}$ − 20.7° (c = 0.20, MeOH); HR-ESI-MS *m/z* 503. 1627 $[M-H]^-$; HR-ESI-MS^2 *m/z* 367.1204 [M-dihydroxy benzoic acid]$^-$, 153.0272 [dihydroxy benzoic acid]$^-$; ^{1}H NMR (400 MHz, d_6-DMSO) and ^{13}C NMR (100 MHz, d_6-DMSO) spectrum information, see Table 2.

Table 1
^{1}H NMR (400 MHz) and ^{13}C NMR (100 MHz) data of compounds **1**, **23**, and **24** in d_6-DMSO.

	Compound **1**			Compounds **23**/**24**	
Position	^{1}H NMR	^{13}C NMR	Position	^{1}H NMR	^{13}C NMR
1		195.37	1		168.29
2	5.72 (s)	125.01	2	7.95 (s)	138.77
3		161.94	3		148.98
4	1.97 (s); 2.43 (m)	44.07	4		144.08
5		84.86	5		141.20
6		38.36	6	2.23 (s)	14.20
7	1.77 (d, 4.7); 2.43 (m)	29.98	7	2.23 (s)	14.20
8	1.90 (d, 4.4); 2.02 (s)	34.32	1′		167.16
9		107.19	2′	5.86 (dd, 15.6, 1.6	119.85
10	3.35 (s); 3.73 (s)	68.98	3′	6.78 (dd, 15.5, 4.6)	151.35
11	1.84 (s)	16.46	4′	4.06 (d, 4.3)	70.23
12	1.14 (s)	19.86	5′	1.45 (m)	29.00
13	1.43 (s)	23.87	6′	0.85 (t, 7.4)	9.47

Table 2
^{1}H NMR (400 MHz) and ^{13}C NMR (100 MHz) data of compound **28** in d_6-DMSO.

	Compound **28**	
Position	^{1}H NMR	^{13}C NMR
1		73.07
2	1.94 (dd, 13.5, 3.0); 2.11(t, 10.6)	35.19
3	3.59 (s)	69.40
4	5.03 (d, 3.3)	70.95
5	3.89 (d, 8.8)	66.94
6	1.78 (dd, 12.5, 9.5); 2.11(t, 10.6)	37.20
7		173.55
OCH_3	3.56 (s)	51.71
1′		125.35
2′	7.03 (s)	115.81
3′		148.42
4′		145.58
5′	6.77 (d, 8.0)	114.57
6′	6.97 (d, 8.0)	121.24
7′	7.39 (d, 15.9)	145.04
8′	6.11 (d, 15.9)	113.87
9′		165.32
1″		112.75
2″		154.04
3″	6.77 (d, 8.0)	117.63
4″	6.95 (d, 8.0)	123.55
5″		149.27
6″	7.16 (d, 2.0)	114.53
7″		171.63

2.5. Relative configurations of new compounds *1*, *23* and *24*

The theoretical calculations of compounds **1**, **23**, and **24** were performed using Gaussian 09 software (Revision C.01, Gaussian, Inc., Wallingford CT, 2010) and configured using GaussView 5.0 (Version 5, Semichem Inc., Shawnee Mission, KS, 2009). The predominant conformers were optimized at the B3LYP/6-31G (d, p) level.

2.6. Anti-hepatoma activity assay in vitro

The HepG 2 cells and SMCC 7721 cells were from the American Type Culture Collection (ATCC, Manassas, USA). All the cells were maintained in DMEM containing 10% FBS (foetal bovine serum, HyClone, Logan, UT) and cultured at 37 °C (5% CO_2, 95% relative humidity). The cytotoxicity assay was performed, according to the MTT method in 96-well microplates [9]. The protein expressions of BCL-2,

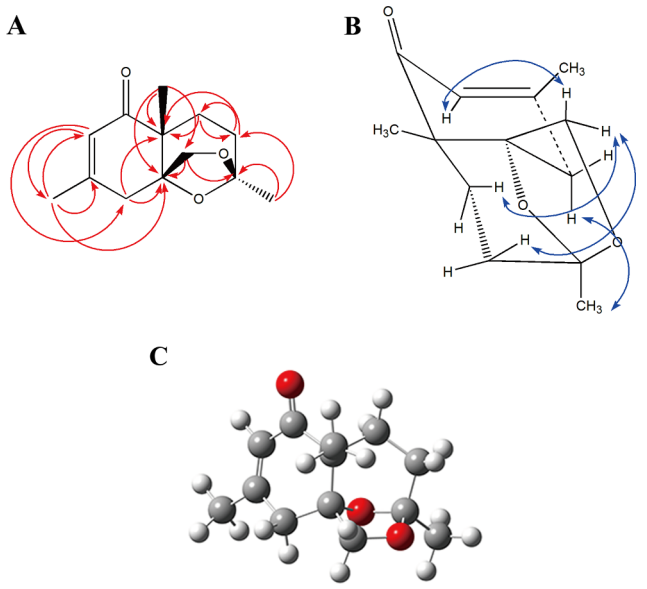

Fig. 3. Structure identification of compound **1**. (**A**) Key HMBC (H → C, red) correlations; (**B**) NOESY (H←→H, blue) correlations; (**C**) Optimized conformation geometry.

BAX, and BAK in SMCC 7721 cells were determined using Western blot analysis [11].

2.7. Anti-HBV activity assay in vitro

HepG 2.2.15 cells were maintained in DMEM containing 10% FBS (foetal bovine serum, HyClone, Logan, UT) and cultured at 37 °C (5% CO_2, 95% relative humidity). The anti-HBV assay was performed according to previous research [10].

2.8. Statistical analysis

All data is expressed as mean ± SD. At least three independent experiments were performed, each in quintuplicate. The data was analysed using a one-way ANOVA. Statistically significant effects were analysed, and the means were also compared using the least-significant difference (LSD) test. Statistical significance was determined at $p < 0.05$.

3. Results and discussion

3.1. Structural elucidation of new compounds (1, 23, 24, 28)

Compound **1** was isolated as a pale-yellow viscous oil. The molecular formula was determined to be $C_{13}H_{18}O_3$ by HR-ESI-MS at *m/z* 223.1324 $[M+H]^+$ (calculated for $C_{13}H_{19}O_3$, 223.1327), as well as ^1H NMR and ^{13}C NMR spectrum (Table 1). The ^{13}C NMR and DEPT spectra indicated 13 carbons, which was consistent with the presence of three methyls, four methylenes (one oxygenated), one methine, and five quaternary carbons (one carbonyl, one olefinic, and two oxygenated carbons). The ^1H NMR and HSQC spectrum displayed 18 directly attached protons, which contained three tertiary methyl groups at δ_H 1.84 (3H, s, H-11), 1.14 (3H, s, H-12), and 1.43 (3H, s, H-13); three methylene groups at δ_H 2.43 (2H, m, H-4a, 7a), 1.97 (1H, s, H-4b), 2.02 (1H, s, H-8a), 1.90 (1H, d, J = 4.4 Hz, H-8b), and 1.77 (1H, d, J = 4.7 Hz, H-7b); two oxygenated methylene protons at δ_H 3.73 (1H, s, H-10a) and 3.35 (1H, s, H-10b); an methine group at δ_H 5.72 (1H, s, H-2). Careful analyses of the ^1H–^1H COSY experiment revealed three spin systems. The first spin system included the signals of an olefinic hydrogen (H-2) and a methylene hydrogen (H-4). The HMBC correlation (Fig. 3A) from H-2 (δ_H 5.72) to C-4 and C-5, from H_{ax}-4 (δ_H 2.43) to C-1 and C-6, and from H_{eq}-4 (δ_H 1.97) to C-1 and C-5, revealed that a 3,5,6-trisubstituted cyclohexanone ring. The second spin system included the signals of two methylene hydrogens (H-7 and H-8). In the HMBC spectrum, the correlations of H-7 with C-6 and C-8, and of H-8 with C-6 and C-7 clearly positioned an epoxy six-member ring bridge across C-5/C-6. The third spin system only included an oxygenated methylene hydrogen signal (H-10). The HMBC correlation from H-10 to C-9, along with the oxygenated nature of C-9 and C-10, revealed that an oxo-bridge should be positioned between C-9 and C-10. In addition, the HMBC correlation from H-10 to C-4, C-5, and C-6, further supported the linkage between C-5 and C-10. Consequently, a detailed examination of the above information indicated the presence of a tricyclic monoterpenoid skeleton with two epoxy rings. Furthermore, three methoxyl groups were attached to C-3, C-6, and C-9 through the observed HMBC correlation of H-11 (δ_H 1.84) to C-2, C-3, and C-5, of H-12 (δ_H 1.14) to C-4, C-5, C-6, and C-10, and of H-13 (δ_H 1.43) to C-8 and C-9. Based on the above data and comprehensive 2D NMR experiments (^1H–^1H COSY, HSQC, and HMBC), the structure of compound **1** was established as shown in Fig. 3A. The relative configuration of the stereogenic centers of **1** was elucidated by ^1H–^1H coupling constants, NOESY results (Fig. 3B) as well as comparison of its physical and spectral data with those of the similar compound. In this way, the relative configurations at all the stereogenic centers in **1** were determined to be 5*R*, 6*S*, and 9*R*. To gain additional evidence for the above assignment of relative stereochemistry, the predominant conformer of compound **1** was calculated by Gaussian 09 software. The optimized conformation geometry was shown in Fig. 3C for its lowest energy, which was consistent with that of the above NMR spectrum. During the ECD test, we observed no Cotton effects when the wavelength were greater than 300 nm. Thus, the ECD spectra with strong Cotton effects were only recorded and the wavelength was 200–300 nm. Furthermore, the electronic circular dichroism (ECD) and UV of the result of the theoretical calculation agrees

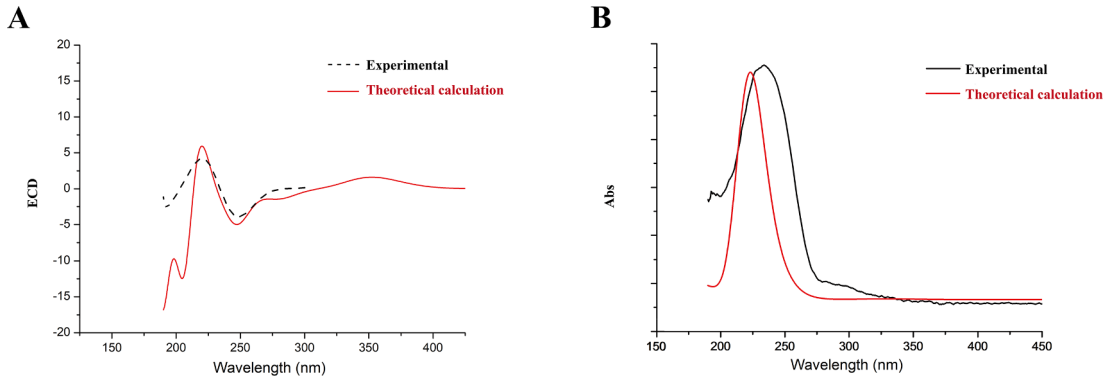

Fig. 4. Calculated and experimental results of compound **1**. (**A**) ECD spectrum; (**B**) UV spectrum.

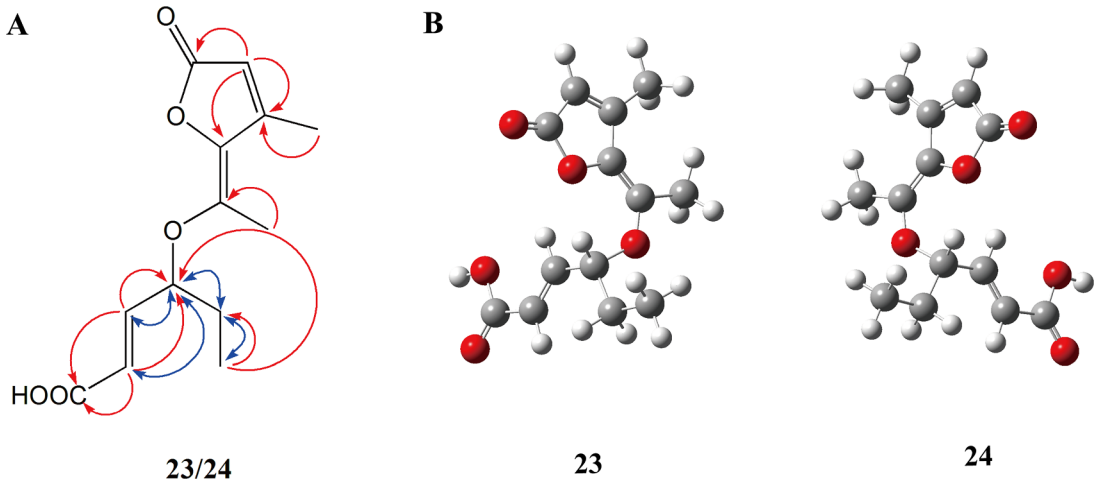

Fig. 5. Structure identification of compounds **23** and **24**. (**A**) Key HMBC (H → C, red) and NOESY (H←→H, blue) correlations; (**B**) Optimized conformation geometry.

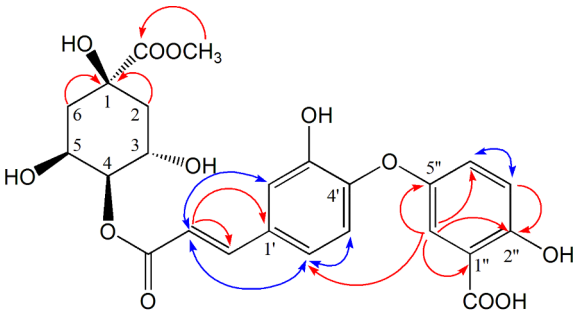

Fig. 6. Key HMBC (H → C, red) and NOESY (H←→H, blue) correlations (H → C, black) of compound **28**.

well with that determined experimentally (Fig. 4, S9 and S10). Thus, compound **1** was assigned as (5*R*, 6*S*, 9*R*)-3,6,9-trimethyl-10,12-dioxatricyclo[7.2.1.0^{1,6}]dodec-3-en-5-one, which was renamed japopenoid A.

Compounds **23** and **24**, isolated as an orange oil, has a molecular formula of $C_{13}H_{16}O_5$ (six unsaturations), which was deduced from the HR-ESI-MS, ^{13}C NMR, and elementary analysis data. The NMR data (Table 1) for **23** and **24** revealed the presence of three methyls, one methylene, one sp^3 oxygenated methine, three sp^2 methines, three quaternary carbons, and two carbonyl carbons, indicating that **23** and **24** have a lactone ring and a fatty acid. The HMBC correlation (Fig. 5A) from H-2 (δ_H 7.95) to δ_C 168.29 (C-1), 148.98 (C-3), and 144.08 (C-4), revealed a disubstituted five-member lactone ring. Considered the quaternary carbon properties of C-3, 4, and 5, a cyclic olefinic bond across C-2/C-3 and an exocyclic double bond across C-4/C-5 were established. In addition, two methoxyl groups were attached to C-3 and C-5 through the observed HMBC correlation of δ_H 2.23 (H-6, 7) to C-3 and C-5, respectively. The other six carbons formed a 4-hydroxy-2-hexenoic acid group, which was linked to C-5. The HMBC correlations (Fig. 5A) observed from H-2′ (δ_H 5.86) to C-1′ and C-4′, from H-3′ (δ_H 6.78) to C-1′ and C-4′, and from H-6′ (δ_H 0.85) to C-4′ and C-5′, furrther confirmed the above conclusion. Meanwhile, the $J_{H\text{-}2', H\text{-}3'}$ value of 15.6 Hz revealed that the geometry of the double bond between C-2′ and C-3′ was *E*. These partial structures were linked on the basis of HMBC data. And the absolute configuration of C-4′ of **23** and **24** were further established to be 4′*R* and 4′*S*, since there is no Cotton effect in the ECD spectrum (see supporting information). In addition, the calculation results performed using Gaussian 09 software showed that 4*S* was the most favored conformation (Fig. 5B). Thus, **23** and **24** are a couple of racemic mixture, determined to be (4*R*)-4-[1-(3-Methyl-5-oxo-5H-furan-2-ylidene)- ethoxy]-hex-2-enoic acid and (4*S*)-4-[1-(3-Methyl-5-oxo-5H-furan-2-ylidene)- ethoxy]-hex-2-enoic acid, renamed japopenoid B and japopenoid C, respectively.

Table 3
Anti-hepatoma activities (IC_{50}) of all compounds (**1–35**).

Compounds	IC_{50} (μg/ml)	
	HepG 2	SMMC 7721
1	174.96 ± 13.33	181.19 ± 6.39
2	140.10 ± 4.03	166.37 ± 8.96
3	54.78 ± 0.53	73.47 ± 2.16
4	144.60 ± 2.02	145.98 ± 2.26
5	47.29 ± 3.27	50.30 ± 1.72
6	181.33 ± 16.66	> 300
7	> 300	> 300
8	> 300	> 300
9	> 300	> 300
10	> 300	> 300
11	104.69 ± 2.21	99.46 ± 5.54
12	26.54 ± 1.95	8.72 ± 1.57
13	26.54 ± 1.95	12.35 ± 1.43
14	143.05 ± 8.01	126.06 ± 2.93
15	> 300	288.35 ± 7.40
16	> 300	> 300
17	188.87 ± 9.09	293.50 ± 0.57
18	> 300	> 300
19	> 300	> 300
20	> 300	173.67 ± 17.84
21	218.08 ± 12.08	212.85 ± 9.77
22	> 300	> 300
23/24	> 300	> 300
25	> 300	> 300
26	157.13 ± 4.25	143.17 ± 5.87
27	> 300	> 300
28	> 300	145.30 ± 12.48
29	> 300	> 300
30	> 300	> 300
31	68.99 ± 7.74	62.80 ± 4.64
32	284.57 ± 17.50	122.73 ± 3.09
33	233.57 ± 13.89	> 300
34	> 300	> 300
35	> 300	> 300
Cisplatin	15.67 ± 2.30	13.26 ± 0.17

Compound **28** was isolated as a green oil, with the molecular formula of $C_{24}H_{24}O_{12}$ as deduced from the $[M-H]^-$ peak at *m/z* 503.1627 (calculated for $C_{24}H_{23}O_{12}$, 503.1627) via HR-ESI-MS and supported by the ^{13}C NMR spectral data. The ^{1}H NMR and ^{13}C NMR spectrum (Table 2) showed the presence of a 4-*O*-*trans*-caffeoylquinic acid methyl ester group, which was confirmed to a quinic acid methyl

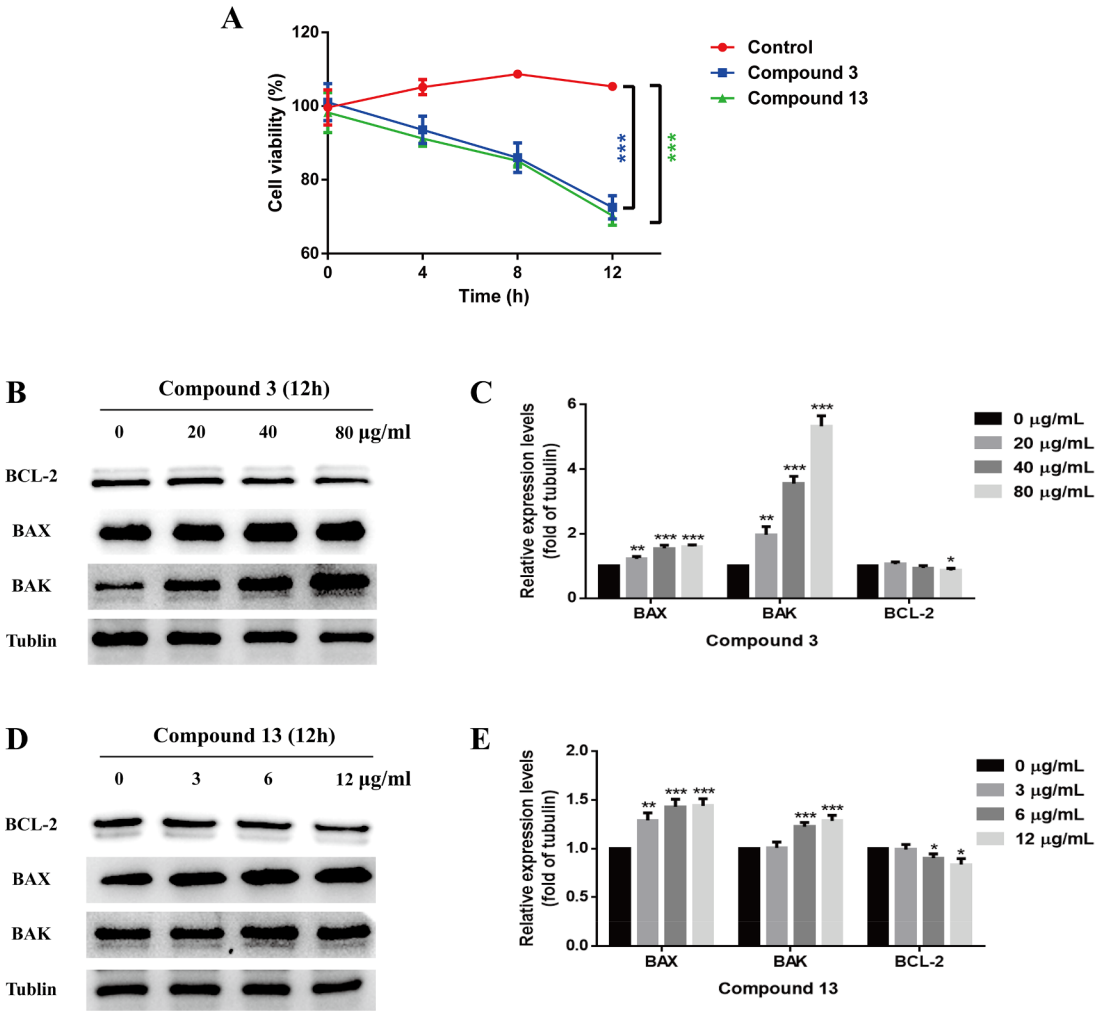

Fig. 7. Compounds **3** and **13** induces hepatoma cell apoptosis. (**A**) Compounds **3** (40 μg/mL) and **13** (6 μg/mL) were exposed to SMMC-7721 for indicated time for the MTT assays to evaluate the cell viability; (**B** and **C**) SMMC-7721 cells treated with different concentrations of compound **3** for 12 h were analyzed and subjected to immunoblotting for detection of the expression levels of relative proteins; (**D** and **E**) SMMC-7721 cells treated with different concentrations of compound **13** for 12 h were analyzed and subjected to immunoblotting for detection of the expression levels of relative proteins. Results are expressed as the mean ± SD (n = 5). $^{*}p < 0.05$ compared with the control group, $^{**}p < 0.01$ compared with the control group, $^{***}p < 0.001$ compared with the control group.

ester moiety [δ_H 5.03 (1H, d, J = 3.3 Hz), 3.89 (1H, d, J = 8.8 Hz), 3.59 (1H, s), 3.56 (3H, s, $-OCH_3$), 2.11 (2H, t, J = 10.6 Hz), 1.94 (1H, dd, J = 13.5, 3.0 Hz), 1.78 (1H, dd, J = 12.5, 9.5 Hz); δ_C 73.07 (C-1), 35.19 (C-2), 69.40 (C-3), 70.95 (C-4), 66.94 (C-5), 37.20 (C-6), 173.55 (C-7), 51.71 (C-OCH_3)] and a trans-caffeoyl moiety [δ_H 7.39 (1H, d, J = 15.9 Hz), 7.03 (1H, s), 6.97 (1H, d, J = 8.0), 6.77 (1H, d, J = 8.0 Hz), 6.11 (1H, d, J = 15.9 Hz); δ_C 125.35 (C-1′), 115.81 (C-2′), 148.42 (C-3′), 145.58 (C-4′), 114.57 (C-5′), 121.24 (C-6′), 145.04 (C-7′), 113.87 (C-8′), 165.32 (C-9′)]. HSQC correlations and HMBC correlations analysis also supported the above speculation. In addition, three aromatic proton signals at δ_H 7.16 (1H, d, J = 2.0 Hz), 6.95 (1H, d, J = 8.0 Hz), and 6.77 (1H, d, J = 8.0 Hz) indicated the presence of a 2,5-dihydroxybenzoyl moiety, which was confirmed according to the observed HMBC correlations of δ_H 7.16 (H-6″) to δ_C 154.04 (C-2″), 123.55 (C-4″), 149.27 (C-5″), 171.63 (C-7″) in Fig. 6. Moreover, the HMBC correlations indicated that the 5″-OH of the 2,5-dihydroxybenzoic acid moiety was linked to the 4′-OH of the caffeoyl moiety through the observed correlations of H-6″ (δ_H 7.16) to 121.24 (C-6′) (Fig. 6). Therefore, compound **28** is 4-*O*-[4′-*O*-5″-(2,5-dihydroxybenzoic acid)-caffeoyl]-quinic acid methyl ester.

The other known compounds were identified as aspertenol B (**2**) [12], balanophonin B (**3**) [13], 7-methoxy-1,2-dihydrocadalene (**4**) [14], syringic aldehyde (**5**) [15], scopoletin (**6**) [16], pinoresinol (7) [17], epipinoresinol (**8**) [18], *p*-hydroxy-benzaldehyde (**9**) [19], 1H-indole-3-carboxaldehyde (**10**) [20], 3-hydroxy-*β*-damascone (**11**) [21], naringenin (**12**) [22], 3,5-dyhydroxy-7-methoxyflavone (**13**) [23], (3*S*)-3,7-dimethyl-3,8-dihydrooctene (**14**) [24], (6*S*), (2*E*)-2,6-dimethyl-6-hydroxyl-2,7-octadienoic acid (**15**) [25], pyrocatechol (**16**) [26], *p*-coumaric acid (**17**) [27], argaminolic A (**18**) [28], esculetin (**19**) [29], protocatechuate (**20**) [30], taxifolin (**21**)[31], (−)-(7*R*,8*S*)-dihydrodehydrodiconiferyl alcohol (**22**) [32], 6-hydroxy-benzyl-benzoate-2-*O*-*β*-D-glucoside (**25**) [33], (1′*R*, 3′*S*, 5′*R*, 8′*S*, 2*Z*, 4*E*)-dihydrophaseic acid (**26**) [34], 1-*O*-caffeoyl glycerides (**27**) [35], benzyl-*O*-*β*-D-glucopyranoside (**29**) [36], secologanin dimethylacetal (**30**) [37], 3-*O*-isorhamnetin 6-*O*-(*p*-coumaroyl)-*β*-D-glucopyranoside (**31**) [38], *epi*-vogeloside (**32**) [39], vogeloside (**33**) [39], 4-*O*-feruloylquinic acid methyl ester (**34**) [40], sweroside (**35**) [41], base on comparisons of their spectral data with the literatures.

3.2. Anti-hepatoma activities in vitro

L. japonica produces many types of secondary metabolites, including flavonoids, terpenoids, phenylpropanoids, caffeoylquinic acid derivatives, alkaloids, and so on. All compounds isolated from *L. japonica* in this study were assayed for their anti-hepatoma activities, and the results are listed in Table 3. Among them, compound **12** exhibited the

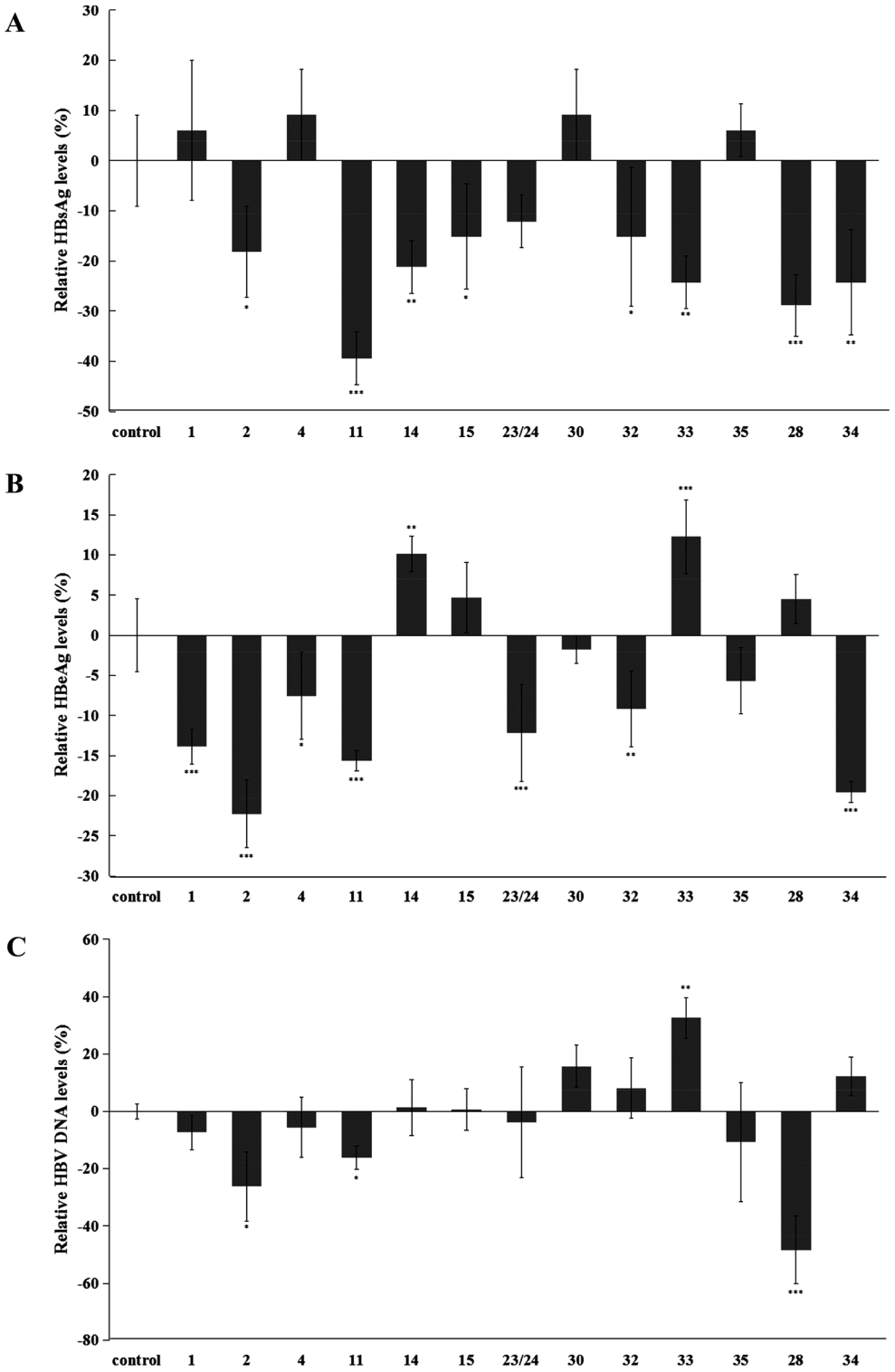

Fig. 8. Anti-HBV activities of terpenes (**1**, **2**, **4**, **11**, **14**, **15**, **23**, **30**, **32**, **33**, and **35**) and caffeoylquinic acid derivatives (**28** and **34**). (**A**) Relative HBsAg levels; (**B**) Relative HBeAg levels; (**C**) Relative HBV DNA levels. The figure shows the results of the experiment on the third day. Compounds **1**, **2**, **4**, and **11** were tested for 25 μg/ml, and the other compounds (**14**, **15**, **23**, **28**, **30**, **32–35**) were tested for 100 μg/ml. Results are expressed as the mean ± SD (n = 3). *$p < 0.05$ compared with the control group, **$p < 0.01$ compared with the control group, ***$p < 0.001$ compared with the control group.

most potent activity with IC_{50} values of 26.54 ± 1.95 and 8.72 ± 1.57 μg/ml against human liver cancer cell lines HepG 2 and SMMC-7721, and compound **13** exhibited significant growth inhibitory effects against HepG 2 and SMMC-7721 with IC_{50} values at 26.54 ± 1.95 and 12.35 ± 1.43 μg/ml, respectively. These values were similar in their anti-hepatoma activities to the positive drug, Cisplatin. Compounds **3**, **7**, **8**, and **22** were phenylpropanoids, which consisted of a kind of natural compound composed of benzene ring and three straight chain carbons (C6-C3). Compounds **7**, **8**, and **22** showed no inhibitory effects against liver cancer cell lines (IC_{50} values > 300 μg/ml), but compound **3** exhibited potent activity with IC_{50} values of 54.78 ± 0.53 and 73.47 ± 2.16 μg/ml against HepG 2 and SMMC-

7721. This could be because the carbonyl carbon from C-9 of compound **3** produced a positive effect on the anti-hepatoma activity assay. Monoterpenoids (**1**, **2**, **4**, **11**, **14**, and **26**) showed moderate anti-hepatoma activities with a IC_{50} values range of 100–200 μg/ml, while iridoids (**30**, **32**, **33**, and **35**) showed no significant cytotoxicity against HepG2 and SMMC-7721 cells. Similarly, caffeoylquinic acid derivatives (**28** and **34**) also showed no significant anti-hepatoma activities. Some observations could be made according to the above results. The anti-hepatoma activity of flavonoids was optimal, followed by phenylpropanoids and terpenoids.

Next, we choose two representative compounds **3** (phenylpropanoid) and **13** (flavonoid) to investigate the mechanism of cell death. As shown in Fig. 7A, the cell viability was significantly dropped in a time-dependent manner after treatment with compound **3** or **13**. The microscopy indicated the massive cell death caused by compound **3** or **13** could to be the typical apoptotic cell death characterized by cell shrinkage, pyknosis, massive plasma membrane blebbing and the destruction of cell fragments into apoptotic bodies [42]. The dependence of caspase activation is a major biochemical feature of apoptosis [43]. To validate the mechanism of cell apoptosis caused by compound **3** or **13**, we assessed the protein levels of several regulators of apoptosis, including anti-apoptotic protein B-cell lymphoma-2 (BCL-2) and pro-apoptotic proteins bcl-2-associated X protein (BAX) and bcl-2 antagonist killer (BAK). The Western blot analysis revealed that compound **3** or **13** significantly reduced the expression of BCL-2 and promoted the expression of BAX and BAK compared with the control group (Fig. 7B, C, D, E). In conclusion, the above data proved that compounds **3** and **13** induce hepatoma cell apoptosis *via* the intrinsic apoptosis pathway.

3.3. Anti-HBV activities in vitro

In our previous study, we found that most caffeoylquinic acids from *L. japonica* flower buds have significant anti-HBV activities [10]. In the anti-HBV study, terpenoids were also active ingredients with inhibiting HBsAg and HBeAg secretion, and HBV DNA replication [44]. In this study, we chose terpenoids and caffeoylquinic acids to evaluate their anti-HBV activities (Fig. 8). As shown in Fig. 8A, compounds **11** and **28** showed significant activities in inhibiting the secretion of HBsAg and their relative HBsAg levels were -39.39 ± 5.25 and $-28.87 \pm 6.19\%$, respectively ($p < 0.001$). The HBeAg results of Fig. 8B showed that the replication rate of HBV was significantly inhibited by compounds **1**, **2**, **11**, **23/24**, and **34**, and their relative HBeAg levels as low as -13.88 ± 2.17, -22.24 ± 4.21, -15.64 ± 1.25, -12.14 ± 6.05, and $-19.59 \pm 1.31\%$, respectively ($p < 0.001$). While HBV DNA is a marker of HBV viral replication and the efficacy of anti-HBV activity [45], compound **28** showed the most significant inhibitory activity and its relative HBV DNA level was decreased by $48.38 \pm 11.81\%$ (Fig. 8C). On the whole, the monoterpenoids (**1**, **2**, **4**, **11**, and **23/24**) and caffeoylquinic acids (**28** and **34**) showed significant anti-HBV activities and iridoids (**30**, **32**, **33**, and **35**) were worse. Interestingly, compound **32** inhibited HBsAg and HBeAg secretion by 15.15 ± 13.87 and $9.12 \pm 4.73\%$ ($p < 0.05$), but its isomer (**33**) promoted HBeAg secretion and HBV DNA replication by 12.27 ± 4.60, and $32.57 \pm 7.20\%$ ($p < 0.01$). Therefore, more studies are necessary to further verify the research.

4. Conclusion

Three new naturally occurring monoterpenoids, japopenoid A (**1**), japopenoid B (**23**) japopenoid C (**24**), and one new caffeoylquinic acid derivative (**28**), together with thirty-one known compounds (**2**–**22**, **25**–**27**, **29**–**35**), were isolated and identified from the flower buds of *Lonicera japonica* Thunb. Compound **1** was a monoterpenoid with an unusual tricyclic skeleton, which occurred rarely in natural products. All compounds (**1**–**35**) were evaluated for their cytotoxicities against human liver cancer cell lines (HepG 2 and SMMC-7721). Flavonoid **12** exhibited the most potent activity with IC_{50} values of 26.54 ± 1.95 and 8.72 ± 1.57 μg/ml against HepG 2 and SMMC-7721, and the IC_{50} values of compound **13** were 26.54 ± 1.95 and 12.35 ± 1.43 μg/ml, respectively. The western blot results further proved that compound **13** induces hepatoma cell apoptosis *via* the intrinsic apoptosis pathway. In addition, most terpenoids showed inhibitory activity against HBsAg and HBeAg secretion, and HBV DNA replication. In particular, 25 μg/ml of compound **11** inhibits HBsAg and HBeAg secretion, and HBV DNA replication by 39.39 ± 5.25, 15.64 ± 1.25 and $16.13 \pm 4.10\%$ compared to the control ($p < 0.05$). These results indicated that *L. japonica* flower buds could be served as functional food for anti-hepatoma and anti-HBV activities. Further studies on the relevant mechanism of the isolated compounds are needed.

Acknowledgements

This work was supported by grants from the National Natural Science Foundation of China (81503221, 81703939), the Guangdong Natural Science Fund (2017A030313659, 2014A030310365), the Shenzhen basic research project (JCYJ20170307095556333, JCYJ20170413093108233, JCYJ20160427183814675, JCYJ20160422152223097), and the China Postdoctoral Science Foundation Grant (2018M633290).

Declaration of Competing Interest

The authors of the present manuscript have declared that no competing interests exist.

Appendix A. Supplementary material

Supplementary data to this article can be found online at https://doi.org/10.1016/j.bioorg.2019.103198.

References

[1] J.F. Perz, G.L. Armstrong, L.A. Farrington, Y.J. Hutin, B.P. Bell, J. Hepatol. 45 (2006) 529–538.
[2] H.B. El-Serag, Clin. Liv. Dis. 5 (2001) 87–107.
[3] E.S. Bialecki, A.M. Di Bisceglie, Eur. J. Gastroen. Hepat. 17 (2005) 485–489.
[4] G. Fattovich, T. Stroffolini, I. Zagni, F. Donato, Gastroenterol. 127 (2004) S35–S50.
[5] H.B. El-Serag, Gastroenterol. 142 (2012) 1264–1273.
[6] M. Ringelhan, T. O'connor, U. Protze, M. Heikenwalder, J. Pathol. 235 (2015) 355–367.
[7] Chinese Pharmacopoeia Commission, Pharmacopoeia of the People's Republic China, 2015 edition; China Medical Science Press, Beijing, China, vol. 1, 2015, pp. 221.
[8] E.J. Lee, J.S. Kim, H.P. Kim, J.H. Lee, S.S. Kang, Food Chem. 120 (2010) 134–139.
[9] L.L. Ge, J.M. Li, H.Q. Wan, K.D. Zhang, W.G. Wu, X.T. Zou, S.P. Wu, B.P. Zhou, J. Tian, X.B. Zeng, Ind. Crop. Prod. 125 (2018) 114–122.
[10] L.L. Ge, H.Q. Wan, S.M. Tang, H.X. Chen, J.M. Li, K.D. Zhang, B.P. Zhou, J. Fei, S.P. Wu, X.B. Zeng, RSC Adv. 8 (2018) 35374–35385.
[11] H.Q. Wan, J.M. Li, K.D. Zhang, X.T. Zou, L.L. Ge, F.Q. Zhu, H.R. Zhou, M.N. Gong, T.W. Wang, D.L. Chen, S.S. Peng, B.P. Zhou, X.B. Zeng, Sci. Rep. 8 (2018) 13152.
[12] L. Liu, R. Liu, B.B. Basnet, L. Bao, J. Han, L. Wang, H. Liu, J. Antibiot. 71 (2018) 538–545.
[13] G.X. Ma, H.F. Wu, J.Q. Yuan, L.Z. Wu, Q.X. Zheng, Z.C. Sun, X.R. Fan, H. Wei, J.S. Yang, X.D. Xu, Phytochem. Lett. 6 (2013) 152–155.
[14] K. Nabeta, K. Katayama, S. Nakagawara, K. Katoh, Phytochem. 32 (1992) 117–122.
[15] Y.R. Li, C. Li, Z.M. Wang, L.X. Yang, Chin. J. Chin. Mater. Med. 39 (2014) 1163–1167.
[16] N.K. Kassim, M. Rahmani, A. Ismail, M.A. Sukari, G.C.L. Ee, N.M. Nasir, K. Awang, Food Chem. 139 (2013) 87–92.
[17] L.Q. Wang, Y.X. Zhao, L. Zhou, J. Zhou, Chem. Nat. Comp. 45 (2009) 424–426.
[18] M.M. Rahman, P.M. Dewick, D.E. Jackson, J.A. Lucas, Phytochem. 29 (1990) 1971–1980.
[19] X.P. Li, W.K. Yuan, J.Y. Li, Y.Q. Tang, Y.L. Deng, X.Q. Liu, Chin. Trad. Herb. Drugs 47 (2016) 388–391.
[20] M.T. Gutierrez-Lugo, G.M. Woldemichael, M.P. Singh, P.A. Suarez, W.M. Maiese, G. Montenegro, B.N. Timmermann, Nat. Prod. Res. 19 (2005) 645–652.
[21] M. Ma, S.G. Bell, W. Yang, Y. Hao, N.H. Rees, M. Bartlam, W.H. Zhou, L.L. Wong, Z.H. Rao, Chem. Bio. Chem. 12 (2011) 88–99.
[22] R. Huang, K.X. Ma, X.S. Xie, T. Wang, S.H. Wu, Chem. Nat. Comp. 51 (2015) 392–394.
[23] S.M. Zhang, R. Li, G.Q. Lin, Youji Huaxue 18 (1998) 259–262.
[24] Y.L. Wang, Y. Li, G.A. Luo, Y.M. Wang, Nat. Prod. Res. Devel. 19 (2007) 51–54.

[25] K. Yoshikawa, Y. Suzaki, M. Tanaka, S. Arihara, S.K. Nigam, J. Nat. Prod. 60 (1997) 1269–1274.
[26] Z.L. Li, X.H. Lv, X.J. Wang, X.J. Zhou, J. Li, S.H. Qian, Chin. Trad. Herb. Drugs 49 (2018) 3226–3231.
[27] Y.C. Zeng, S.Y. Liang, J.H. Wu, Z.Q. Li, Z.Z. Wu, Chin. Trad. Pat. Med. 40 (2018) 1768–1772.
[28] F. Khallouki, J. Voggel, A. Breuer, K.D. Klika, C.M. Ulrich, R.W. Owen, Food Chem. 221 (2017) 1034–1040.
[29] X. Lu, Y. Qiao, X. Zhang, B. Ma, M. Qiu, Acta Botan. Yunnan. 29 (2007) 263–264.
[30] Y. Huang, X. Wu, J.W. Wen, M.S. Chen, K.J. He, B.M. Liu, Chin. Trad. Herb. Drugs 47 (2016) 3159–3163.
[31] L. Pistelli, I. Giachi, D. Potenza, I. Morelli, J. Nat. Prod. 63 (2000) 504–506.
[32] Y.P. Jiang, Y.F. Liu, Q.L. Guo, C.B. Xu, S. Lin, C.G. Zhu, Y.C. Yang, J.G. Shi, Acta Pharm. Sin. 51 (2016) 616–625.
[33] C.C. Zhou, C.T. Liu, X.X. Huang, J. Wu, L.Z. Li, D.M. Li, S.J. Song, Chin. J. Med. Chem. 23 (2013) 213–217.
[34] L. Cai, C.S. Liu, X.W. Fu, X.J. Shen, T.P. Yin, Y.B. Yang, Z.T. Ding, Nat. Prod. Bioprosp. 2 (2012) 150–153.
[35] P. Wang, J. Xu, Q. Wang, S.X. Feng, T. Chen, C.L. Zhang, Chin. J. Chin. Mater. Med. 38 (2013) 1531–1535.
[36] S. De Marino, C. Festa, F. Zollo, M. Iorizzi, Phytochem. Lett. 2 (2009) 130–133.
[37] R. Kakuda, M. Imai, Y. Yaoita, K. Machida, M. Kikuchi, Phytochem. 55 (2000) 879–881.
[38] G. Romussi, G. Bignardi, C. Pizza, Eur. J. Org. Chem. 10 (1988) 989–991.
[39] H. Kawai, M. Kuroyanagi, A. Ueno, Chem. Pharm. Bull. 36 (1988) 3664–3666.
[40] Y.P. Li, D.D. Li, L.Q. Ding, F. Qiu, Chin. Trad. Herb. Drugs 47 (2016) 2621–2626.
[41] J.Q. Yu, Z.P. Wang, H. Zhu, G. Li, X. Wang, Acta Pharm. Sin. 51 (2016) 1110–1116.
[42] S. Elmore, Toxicol. Pathol. 35 (2007) 495–516.
[43] M.O. Hengartner, Nat. 407 (2000) 770–776.
[44] Z.Y. Jiang, C.G. Huang, H.B. Xiong, K. Tian, W.X. Liu, Q.F. Hu, H.B. Wang, G.Y. Yang, X.Z. Huang, Tetrahed. Lett. 54 (2013) 3886–3888.
[45] C.J. Chen, H.I. Yang, J.U.N. Su, C.L. Jen, S.L. You, S.N. Lu, G.T. Huang, U.H. Iloeje, Jama 295 (2006) 65–67.